Biosystems Diversity

ISSN 2519-8513 (Print)
ISSN 2520-2529 (Online)
Biosyst. Divers.

Anatomical identification and diagnostic characteristics of *Tragopogon pratensis* (Asteraceae) within the flora of Azerbaijan

A. Sardarova

Azerbaijan State Agricultural University, Ganja, Azerbaijan

Article info

Received 19.06.2025
Received in revised form 20.07.2025
Accepted 24.08.2025

Azerbaijan State Agricultural University, Ozan st., Ganja, AZ2007, Azerbaijan. Tel.: +994-604-44-42. E-mail: aygun.sardarova4442@gmail.com

Sardarova, A. (2025). Anatomical identification and diagnostic characteristics of Tragopogon pratensis (Asteraceae) within the flora of Azerbaijan. Biosystems Diversity, 33(3), e2545. doi:10.15421/012545

The study of plant anatomical structures plays a crucial role in their taxonomic identification and the determination of diagnostic characteristics. Such research facilitates accurate species recognition, clarification of systematic positions, and contributes to the scientific foundation of floristic studies. Due to the limited anatomical data available for *Tragopogon pratensis* L. in the flora of Azerbaijan, this study provides a novel contribution to science by identifying specific anatomical criteria for the species' identification. It represents the first comprehensive investigation of the specific anatomical structures of *T. pratensis* in Azerbaijan and determines its diagnostic features. Both generative and vegetative organs of *T. pratensis* were used as study material. Anatomical, microscopic, histochemical, and biometric methods were employed. Transverse sections from the plant's generative and vegetative organs were treated with reagents, converted into permanent slides, and the results of the microscopic analyses were statistically validated. Anatomical analysis revealed active development of aerenchyma tissue in the bracts, as well as in the leaf blade and leaf base. Distinct types of trichomes were recorded on the abaxial epidermis of both the bracts and the ligules. Specific structural characteristics were analyzed in the stamens and pistils. In the peduncle and stem, well-developed aerenchyma in the pith and schizogenous secretory cavities in the perimedullary region were observed. Endogenous laticifers were identified in transverse sections of both generative and vegetative organs. Vacuolization of ergastic and constitutional substances was detected in the mechanical, dermal, and ground tissues of *T. pratensis*. For the first time, a pseudoisolateral leaf structure was identified in this species within the Azerbaijani flora. In the rosette and primary root, the vascular system elements showed a predominantly radial arrangement, with parenchymatous tissues being dominant overall. In the transverse section of the lateral root, pigmentation was observed in the cell walls of the endodermis. The vascular system exhibited a radial arrangement within the central cylinder. This research demonstrates species-specific anatomical criteria for *T. pratensis* in the Azerbaijani flora and offers both scientific and practical contributions to the field of plant anatomy. Additionally, the findings provide valuable input for the pharmacognostic disciplines of microscopy and phytochemistry, serving as significant markers in the formation and standardization of medicinal plant raw material resources.

Keywords: laticifer; schizogenous secretory canal; pseudoisolateral leaf; anomocytic stomata; trichome; aerenchyma.

Introduction

A comprehensive analysis of floristic elements is essential for understanding plant diversity and clarifying the systematic position of taxa. Such studies contribute significantly to the refinement of taxonomic data, the evaluation of regional floristic richness, biodiversity conservation, and the expansion of scientific data resources. Investigating the anatomical structure of plants is of major scientific importance in terms of taxonomic identification, elucidating ecological adaptation mechanisms, and the efficient utilization of plant resources. Anatomical data enable the identification of diagnostic traits based on internal structures, refinement of phylogenetic relationships, and the examination of environmental factors affecting plant organs. This approach is also vital for the conservation of phytogenetic resources, biodiversity assessment, and the identification of potential medicinal plant species. Hence, such studies make substantial contributions to botany by enhancing plant systematics, explaining adaptive anatomical changes, and scientifically evaluating biomorphological variations.

Species of the genus *Tragopogon* (Asteraceae) have undergone a long evolutionary history and are widely distributed across Eurasia, North Africa, Eastern Europe, and Western Asia (Bell et al., 2012; Soltis et al., 2023). *Tragopogon pratensis* is one such species that is naturally widespread across various regions of the Republic of Azerbaijan.

Tragopogon pratensis is a biennial herbaceous plant characterized by long, lanceolate leaves that are sessile and attached directly to the rosette or stem via the leaf base. At the upper end of the stem, numerous small flowers form a capitulum, with yellow ligulate petals borne on peduncles. The base of the capitulum is surrounded by green bracts. The species has a well-developed taproot system that penetrates deeply into the soil.

Research into the therapeutic properties of *T. pratensis* has revealed that the plant is rich in antioxidants such as polyphenols and flavonoids. Extracts from the plant have shown positive effects on the liver and pancreas, suggesting potential use in the treatment of diabetes (Rotaru et al., 2020). Other studies conducted on related species within the genus *Tragopogon* have demonstrated that leaf extracts may exhibit strong antioxidant, antibacterial, and antifungal activities (Uysal et al., 2019; Dursun et al., 2025). Additionally, several species have been reported to possess antitumor, anti-inflammatory, antihyperlipidemic, and wound-healing effects, and are used in traditional medicine as well as in food (Abdalla & Zidorn, 2020). These pharmacological perspectives highlight the relevance of incorporating anatomical studies for a deeper understanding of this species.

Numerous anatomical studies have been conducted on various plant species across different geographical regions (Liu et al., 2020; Sosnovsky et al., 2021), including comparative analyses of anatomical structures (Ma et al., 2012; Belaeva & Butenkova, 2018; Bezerra et al., 2020; Gao et al., 2023).

Plant anatomy has always remained a focal point of both classical and modern scientific approaches (Lata et al., 2021; Simioni et al., 2023; Talebi et al., 2025). In recent years, studies encompassing the anatomy and morphology of both vegetative and generative organs have gained increasing relevance and are now well-represented in international scientific databases. Leaves, as vital vegetative assimilation organs with great significance for both plants and humans, are the subject of extensive anatomical research across different populations and countries (Makruf et al., 2024; Ramasar et al., 2025; Sevgi et al., 2025). These investigations yield results of both scientific and practical value for modern plant anatomy. Contemporary studies on the anatomy of generative organs are considered particularly relevant,

and research in this area continues to expand (Poli et al., 2017; Lv et al., 2024).

The study of anatomical adaptations in plants is crucial not only for understanding ecological adaptation mechanisms but also for clarifying taxonomic differentiation and phylogenetic relationships. Globally, the contributions of leading scientists in this field are reflected in the significant advancements in botanical sciences (Aydın et al., 2013; Shahrestani et al., 2020; Kumar et al., 2023). Several studies conducted by the author in this direction also hold considerable importance (Sardarova, 2024, 2025a, 2025b).

Despite the medicinal importance of *T. pratensis*, anatomical identification and documentation of its diagnostic structural features within the flora of Azerbaijan remain limited. Studying its anatomical features is crucial for determining its precise taxonomic position and understanding its adaptation strategies under ecological conditions. The findings of this study provide foundational data for assessing the richness of Azerbaijan's flora, conserving biodiversity, and scientifically identifying ethnobotanically significant species.

Materials and methods

Microscopic analyses were conducted on vegetative and generative organs of *Tragopogon pratensis* collected from the Lachin region of the Republic of Azerbaijan (39°38'03" N, 46°33'28" E). The plant materials were initially stabilized using appropriate fixation techniques and subsequently processed under laboratory conditions. During infiltration and sectioning, paraffin (BW Blended Waxes, Inc., US) was used as a supporting medium. The section thickness was calibrated and measured using the micrometric adjustment screw on a microtome. Sections obtained with the microtome were cut at 7, 8, and 9 µm thicknesses under controlled conditions. Following sectioning, differential staining was performed using histochemical methods with specific reagents such as Safranin O (KimyaLab, Turkey), Fast Green, Sudan III, Toluidine Blue, Phloroglucinol-HCl, and Methylene Blue (Innovating Science, US). Additional reagents including xylene, carboxylol, and ethylene (Mir Nauki, Russia) were extensively used throughout the staining process. The selective staining of tissue components was performed in a stepwise manner using a decolorization technique (Pradhan Mitra & Loqué, 2014; Bozdağ et al., 2016; Da Silva et al., 2020; Engin et al., 2024). The sequential use of various histological staining methods allowed a more precise characterization of the anatomical structural components of the *T. pratensis* plant. Permanent slides were prepared using Canada balsam (Innovating Science, US), by placing a drop on a glass slide (AmScope, USA) and covering it with a coverslip. The slides were then incubated at a stable temperature (20–25 °C) until the balsam was fully cured. Permanent slides of transverse sections were subjected to microscopic analyses following complete preparation.

Microscopic examinations were carried out in the laboratory of the Department of Biology at Azerbaijan State Agricultural University using a "Carl Zeiss, Axio Imager A2" microscope (ZEISS, Germany) equipped with LED illumination and specialized objectives (4×, 10×, 40×, 60×, 100×) designed to minimize optical aberrations. An LCD Digital Microscope NLCD-307B model (Wincom Company Ltd., China) was also employed to monitor staining quality and section integrity prior to permanent slide preparation. Final analyses, image capture, and acquisition of micrometric data were conducted using the Carl Zeiss Axio Imager A2. Observations at 100× magnification were enhanced using immersion oil (RMY, US), which increased optical resolution and improved image clarity and contrast. Stereomicroscopes including the Zeiss Stemi 508 (ZEISS, Germany) and Stereo YK-SM067B2 (Wincom Company Ltd., China) were also used for macroscopic examination of the specimens.

To ensure the accuracy of micrometric measurements obtained from microscope images, both eyepiece and stage micrometers (Muhva, China) were used. Calibration of the eyepiece micrometer was first performed with the stage micrometer, after which size estimations of observed structures were calculated based on calibrated scales (Moyo et al., 2015). Additionally, a digital micrometer (Jiavarry, China) was used to record the macroscopic dimensions of the sampled organs. All measurements were properly annotated on corresponding photomicrographs (Jambor et al., 2021).

Herbarium specimens of the pharmacologically important *T. pratensis* were prepared following standard systematic methods, ensuring a comprehensive analysis of the species' anatomy and ecology. These specimens are stored in the herbarium collection of the Department of Biology at Azerbaijan State Agricultural University, named after Academician Valida Tutayuq, and are available for research, education, and reference purposes in botanical and pharmacognostic studies.

Sections from vegetative organs of 15 individuals belonging to the same population were prepared, and the most representative ones were used to create permanent slides for further analysis. Generative organ sections were also examined. Micrometric data obtained during the study were statistically analyzed using Jamovi software (version 2.6.26, University of Sydney, Australia). All quantitative values are expressed as mean ± standard error (SE).

Results

Bract. In *T. pratensis*, aerenchyma tissue is present in the subepidermal adaxial region of the bract. The aerenchyma is delimited from below and structurally supported by groups of parenchyma cells, which also form the septa between aerenchymatous spaces. These parenchyma cells are rich in chloroplasts, indicating active photosynthetic potential. A centrally located large vascular bundle is observed within the bract, accompanied by smaller lateral collateral bundles situated toward the marginal zones. Below the vascular bundles, particularly toward the abaxial epidermis, a layer of parenchyma composed of large, rounded cells is present (Fig. 1; Table 1). Laticifer cells were identified both at the boundary of the phloem tissue and interspersed within the parenchyma cells. The presence of laticifers is considered an anatomical feature supporting the phytotherapeutic properties of the plant. Microscopic anatomical analysis revealed both non-glandular and glandular trichomes on the abaxial epidermis of the bract. The epidermal surface is covered by a well-developed cuticle layer, which serves a protective function against environmental stressors.

Table 1
Quantitative characteristic of the bract of *T. pratensis* (n = 15)

Indicators	Mean + SE
Height of the central vascular bundle	95.76 ± 3.99
Diameter of xylem vessels	9.88 ± 1.90
Thickness of the parenchyma region below the central vascular bundle	195.52 ± 7.98
Diameter of parenchyma cells	35.27 ± 6.70
Height of upper epidermal cells	19.14 ± 4.38
Height of lower epidermal cells	20.25 ± 4.33
Diameter of aerenchyma spaces in the upper subepidermal region	38.08 ± 13.04
Diameter of chlorenchyma cells	26.66 ± 6.60

Note: SE – standard error; all measurements are given in micrometers (µm).

Ligule. The ligule sample was examined microscopically without sectioning. Although the fusion of five petals to form the ligule is clearly observable macroscopically, this feature is more distinctly confirmed at the tissue level under microscopic observation. Micrographic images revealed that the ligule contains six longitudinally aligned vascular bundles. Except for the two marginal bundles, the remaining four bifurcate in the apical region of the ligule. These branches merge pairwise within the lobes at the apex. In these apical regions, xylem vessels with relatively large diameters were observed to be arranged in a disorganized manner. Along the margins of the apical lobes, rounded epidermal cells were noted, while elongated epidermal cells were distributed along the surface of the ligule (Fig. 2; Table 2). These epidermal cells were rich in chromoplasts, contributing to the yellow pigmentation of the ligule. Microscopic analysis also revealed the presence of stomata and trichomes on the adaxial surface of the ligule. The stomata were identified as being of the anomocytic type, with kidney-shaped guard cells and clearly visible open stomatal pores. Long, multicellular trichomes with rectangular-shaped cells arranged in a single row were also observed.

Table 2
Quantitative characteristic of the ligule of *T. pratensis* (n = 15)

Indicators	Mean + SE
Height of epidermal cells at the apical part of the ligule	30.80 ± 3.22
Length of epidermal cells at the middle part of the ligule	89.45 ± 24.49
Width of epidermal cells at the middle part of the ligule	11.81 ± 2.70
Length of stomata	30.08 ± 1.80
Width of stomata	22.62 ± 0.78
Width of trichomes	16.73 ± 1.82

Note: see Table 1.

Pistil. The pistil was examined microscopically to assess its general anatomical structure. Two vascular bundles extending along the length of the pistil were detected. It was evident from the microscopic view that the pistil consists of two carpels and a bifurcated style, each branch leading to a separate stigma, with one vascular bundle per stigma (Fig. 3; Table 3). Within the epidermal cells of the style and stigma, droplet-shaped, light-yellow fluid accumulations were observed, which are likely indicative of biologically active compounds characteristic of the medicinally valuable *T. pratensis*. These epidermal cells exhibit distinctive structural features, forming upwardly directed oval-shaped protrusions along the style surface. In the branching zone and on the stigma surface, these protrusions become more pointed. Numerous pollen grains were observed adhered to the epidermis of the stigma.

Table 3
Quantitative characteristic of the pistil of *T. pratensis* (n = 15)

Indicators	Mean + SE
Width of style	334.34 ± 14.61
Width of stigma	161.61 ± 5.98

Note: see Table 1.

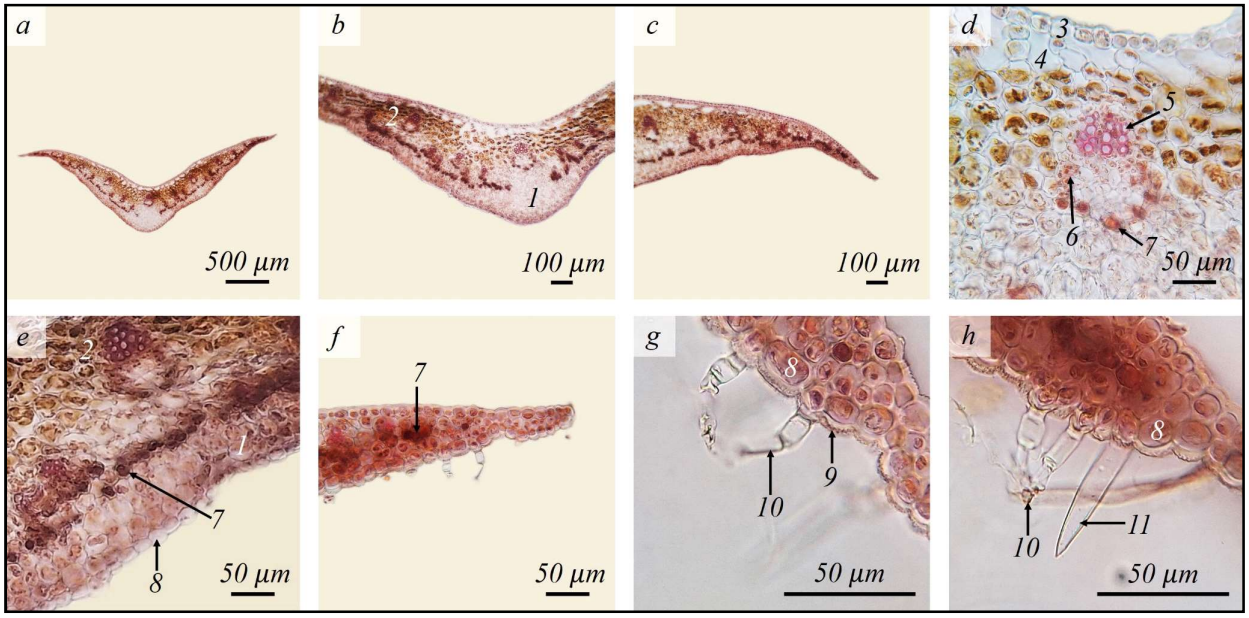

Fig. 1. Transverse section of bract (section thickness: 9 µm): *a* – general view of bract, *b*, *c* – central and lateral parts, *d* – central vascular bundle area, *e* – a part of the bract with lateral vascular bundles, *f* – marginal parts of the bract, *g*, *h* – trichomes on the lower epidermis at the margins; *1* – parenchyma, *2* – chlorenchyma, *3* – upper epidermis, *4* – aerenchyma, *5* – xylem, *6* – phloem, *7* – laticifers, *8* – lower epidermis, *9* – cuticle, *10* – glandular trichome, *11* – non-glandular trichome

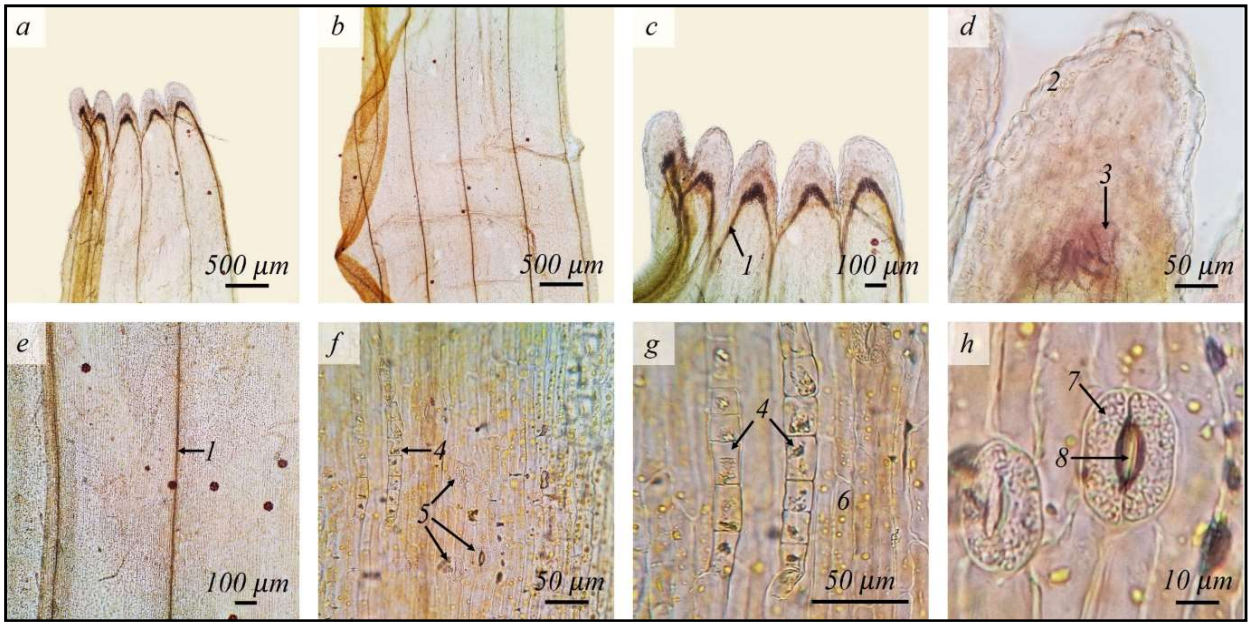

Fig. 2. Microscopic structure of ligule: *a*, *b* – general view of the ligule, *c* – ligule's lobed apical part, *d* – a lobe at the apical region, *e* – middle region of the ligule, *f* – lower epidermis, *g* – trichomes on the lower epidermis, *h* – structure of the stomata; *1* – vascular bundle, *2* – epidermis, *3* – xylem vessels, *4* – multicellular trichomes, *5* – stomata, *6* – lower epidermis cell, *7* – guard cell, *8* – stomatal pore

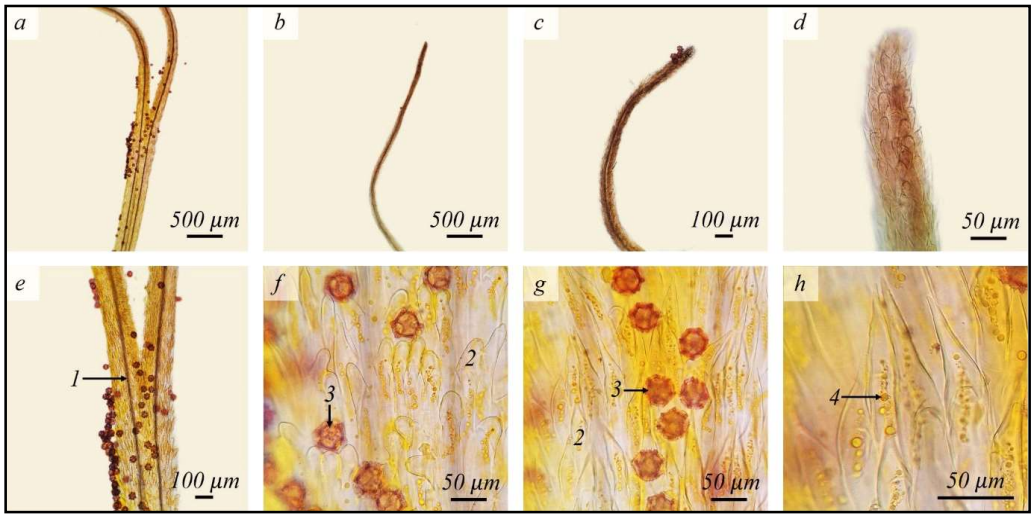

Fig. 3. Microscopic structure of pistil: *a* – general view of the pistil, *b*, *c*, *d* – structure of the bilobed stigma, *e* – starting point of the bilobed stigma from the style, *f* – epidermal cells of the style and the pollen grains adhering to them, *g* – epidermal cells of the stigma and the attached pollen grains, *h* – microscopic characteristics of the stigma's epidermal cells; *1* – vascular bundle, *2* – epidermis cell, *3* – pollen grain, *4* – biological active substrances

Stamen. Microscopic analysis was conducted to study the general structure of the stamens and pollen grains. Each stamen comprises an elongated anther situated on a short filament. The filament was slightly thickened at the point of attachment to the anther. Epidermal cells covering this area were relatively small and clearly visible under the microscope. Each filament contains a single vascular bundle, which extends into the connective tissue at the point of fusion with the anther. The connective tissue joins the two elongated thecae of the anther. A specialized apical appendage formed by the connective tissue was observed at the top of the anther. Microscopic images revealed the presence of thick-walled endothecium cells within the anther. Pollen grains were seen in clusters, adhering to one another along the length of the anther. The surface of the pollen grains exhibits distinctive ornamentation. At the thickened corners of the exine layer, spine-like protrusions (spine-bearing ridges) were detected (Fig. 4; Table 4). Pollen grains were oblate-spheroidal in equatorial view and hexagonal in polar view.

Peduncle. In cross-sections of the peduncle, a central air cavity was observed and identified as aerenchyma. This central air space is surrounded by pith parenchyma cells, which form a continuous layer around it. Vascular bundles are arranged radially around the pith, with a total of 32 vascular bundles observed, of which 13 are large in size. Microscopic analysis revealed schizogenous-type secretory canals located near the xylem elements within these large vascular bundles (Fig. 5; Table 5). These endogenously formed secretory structures indicate localized sites of biologically active compound accumulation and reflect high metabolic activity, as confirmed by micrographic observations. Chloroplast-containing parenchyma cells were also found surrounding the vascular bundles. Protosclerenchyma formation was detected adjacent to the vascular bundles, toward the cortex, with associated laticifer cells observed along its margins. The epidermal cells of the peduncle exhibit thickened outer periclinal walls and are covered by a well-developed cuticle layer. Small trichomes were present on the epidermis. Both the epidermis and underlying parenchyma cells showed accumulation of constitutional substances based on microscopic observations.

Table 4
Quantitative characteristic of the stamen of *T. pratensis* (n = 15)

Indicators	Mean + SE
Width of the anther	463.32 ± 31.88
Polar diameter of the pollen grains	31.30 ± 1.76
Equatorial diameter of the pollen grains	36.06 ± 1.50

Note: see Table 1.

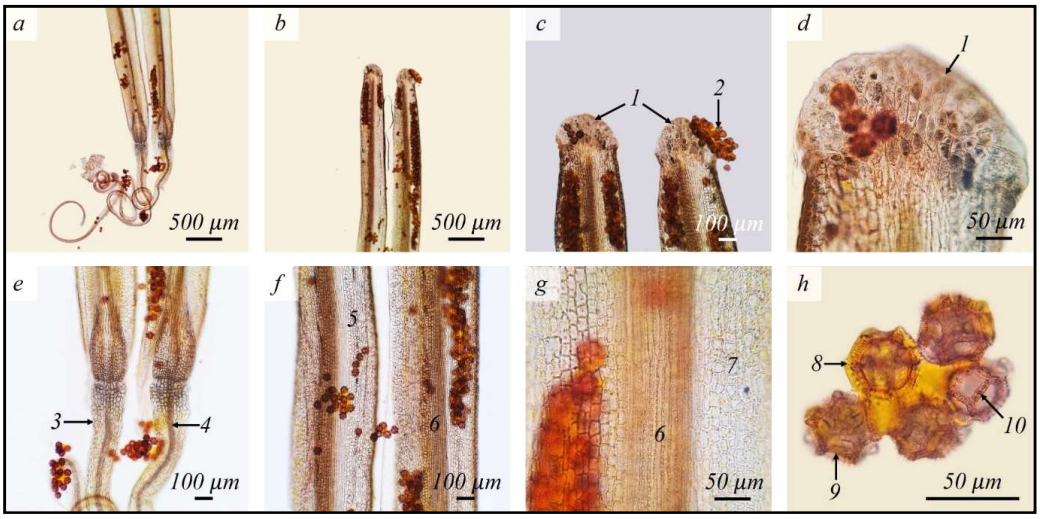

Fig. 4. Microscopic structure of stamen: *a*, *b* – general view of the stamen, *c* – apical part of the stamens and the anther appendages, *d* – appendage at the tip of the anther, *e* – the basal part of the stamens and the filaments attached to the anthers, *f* – central part of the stamens, *g* – connective tissue between the two thecae, *h* – microscopic view of the pollen grains; *1* – appendages, *2* – pollen grains, *3* – filament, *4* – vascular bundle, *5* – thecae, *6* – connective, *7* – endothecial cells, *8* – pollen grain in equatorial view, *9* – pollen grain in polar view, *10* – spine-bearing ridge

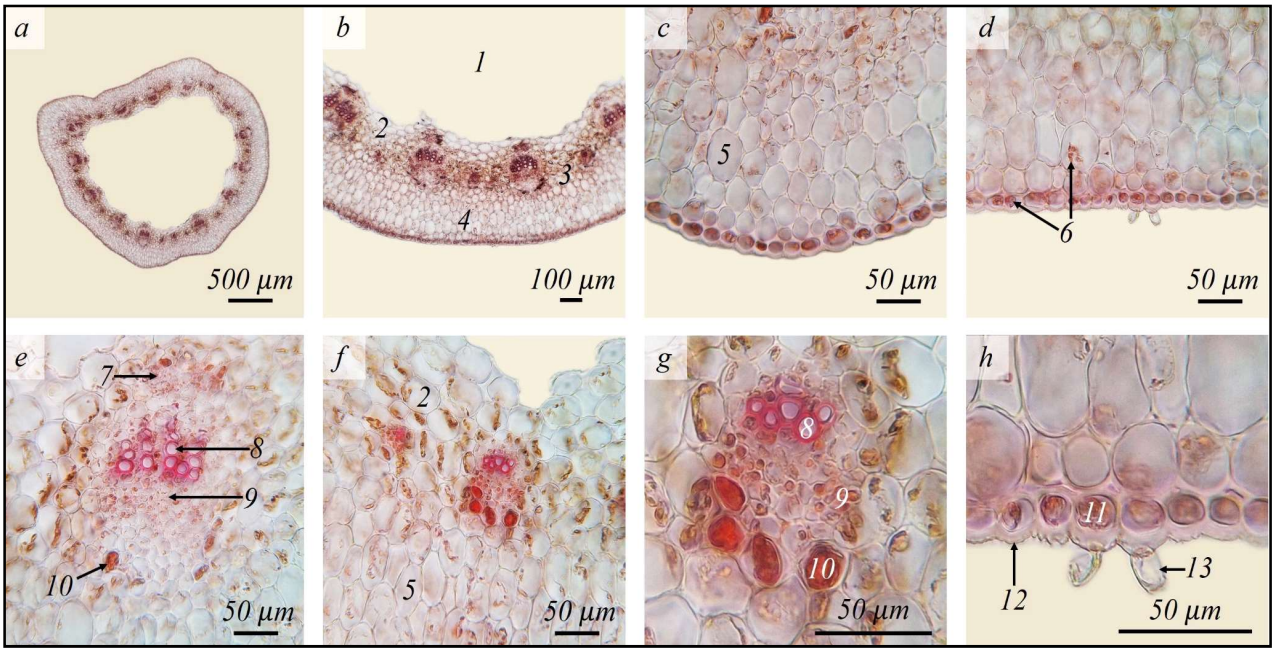

Fig. 5. Transverse section of peduncle (section thickness: 9 μm): *a* – general view of the peduncle, *b* – a part of the peduncle, *c*, *d* – cortex, *e*, *f*, *g* – structure of vascular bundles, *h* – strichomes on the epidermis; *1* – pith cavity, *2* – pith parenchyma cells, *3* – chlorenchyma, *4* – cortex, *5* – cortical parenchyma cells, *6* – constitutional substances, *7* – schizogenous secretory canal, *8* – xylem, *9* – phloem, *10* – laticifers, *11* – epidermis, *12* – cuticle, *13* – trichomes

Table 5
Quantitative characteristic of the peduncle of *T. pratensis* (n = 15)

Indicators	Mean + SE
Thickness of the cortex	179.63 ± 19.52
Diameter of cortex parenchyma cells	38.41 ± 10.48
Height of large vascular bundles	131.61 ± 7.90
Diameter of xylem vessels	12.63 ± 1.30
Height of epidermal cells	19.95 ± 4.98
Diameter of schizogenous secretory canal	49.52 ± 6.36

Note: see Table 1.

Leaf blade. As a result of this study, conducted for the first time within the flora of Azerbaijan, it was determined that the leaf lamina of *T. pratensis* exhibits a pseudoisolateral structure. The formation of weakly developed palisade-like cells and the preservation of adaxial symmetry were interpreted as structural identification traits of the species. Thus, the formation of the pseudoisolateral structure is considered a specific feature of the plant, reflecting the characteristics of its population. In the midrib region of the leaf lamina, the development of aerenchyma structures was observed. Surrounding the aerenchyma, parenchyma cells are located (Fig. 6, Table 6). Pigmentation was observed in the cell walls of those parenchyma cells bordering the aerenchyma cavity. Collenchyma tissue was present on the abaxial side, especially near the corners and beneath large lateral vascular bundles. These were accompanied by chloroplast-rich parenchyma. Vascular bundles were clearly delimited from adjacent parenchyma by bundle sheath cells. On the abaxial side of large bundles, protosclerenchyma was observed adjacent to the phloem, and this region exhibited intensive development of laticifer cells. The outer periclinal walls of both adaxial and abaxial epidermal cells were moderately thickened and covered with cuticle. Anatomical observations also revealed the accumulation of constitutional substances in both epidermis and collenchyma cells. The leaf is amphistomatic in type.

Leaf base. In the basal region of the leaf, inter-bundle areas are filled with large, chloroplast-free parenchyma cells (Fig. 7, Table 7). Aerenchyma formation was prominent in the parenchymatous layer toward the adaxial side. Vascular bundles appeared compact and collaterally arranged. Sclerenchyma tissue was located adjacent to the xylem, while laticifer cells developed prominently around the phloem. Schizogenous secretory canals were observed above the central and lateral large vascular bundles. Subepidermal collenchyma tissue developed on the abaxial side of these regions. The accumulation of constitutional substances was also recorded in collenchyma and both adaxial and abaxial epidermal layers.

Table 6
Quantitative characteristic of the leaf blade of *T. pratensis* (n = 15)

Indicators	Mean + SE
Dorsoventral diameter of aerenchyma space in the midrib region	351.63 ± 7.96
Diameter of parenchyma cells in the midrib region	66.09 ± 14.21
Thickness of collenchyma tissue on the abaxial side in the midrib region	116.19 ± 7.96
Thickness of the leaf lamina	174.05 ± 9.98
Height of adaxial epidermal cells	21.69 ± 1.76
Height of abaxial epidermal cells	22.75 ± 1.70
Diameter of chlorenchyma cells	19.25 ± 3.79
Height of the central vascular bundle	225.75 ± 9.04
Diameter of xylem vessels	29.68 ± 5.74

Note: see Table 1.

Table 7
Quantitative characteristic of the leaf base of *T. pratensis* (n = 15)

Indicators	Mean + SE
Height of adaxial epidermal cells	25.74 ± 1.89
Width of adaxial epidermal cells	32.89 ± 3.68
Height of abaxial epidermal cells	19.91 ± 3.03
Width of abaxial epidermal cells	21.77 ± 9.39
Diameter of parenchyma cells	51.81 ± 17.75
Height of large vascular bundles	351.34 ± 9.28
Diameter of xylem vessels	26.94 ± 5.80

Note: see Table 1.

Stem. Microscopic observations of the stem revealed the presence of a large central aerenchyma cavity. Schizogenous-type secretory canals were present near the perimedullary region, adjacent to large vascular bundles (Fig. 8, Table 8). Sclerenchyma tissue development around the xylem was observed, and the accumulation of ergastic substances in some cells was noted. Laticifer cells were located on the cortical side of the vascular bundles. The subepidermal cortex was composed of alternating layers of chloroplast-rich parenchyma and collenchyma tissues. Deeper into the cortex, larger parenchyma cells devoid of chloroplasts were present. Stomata were observed on the stem epidermis, whose outer periclinal walls were thickened and covered by a cuticle layer.

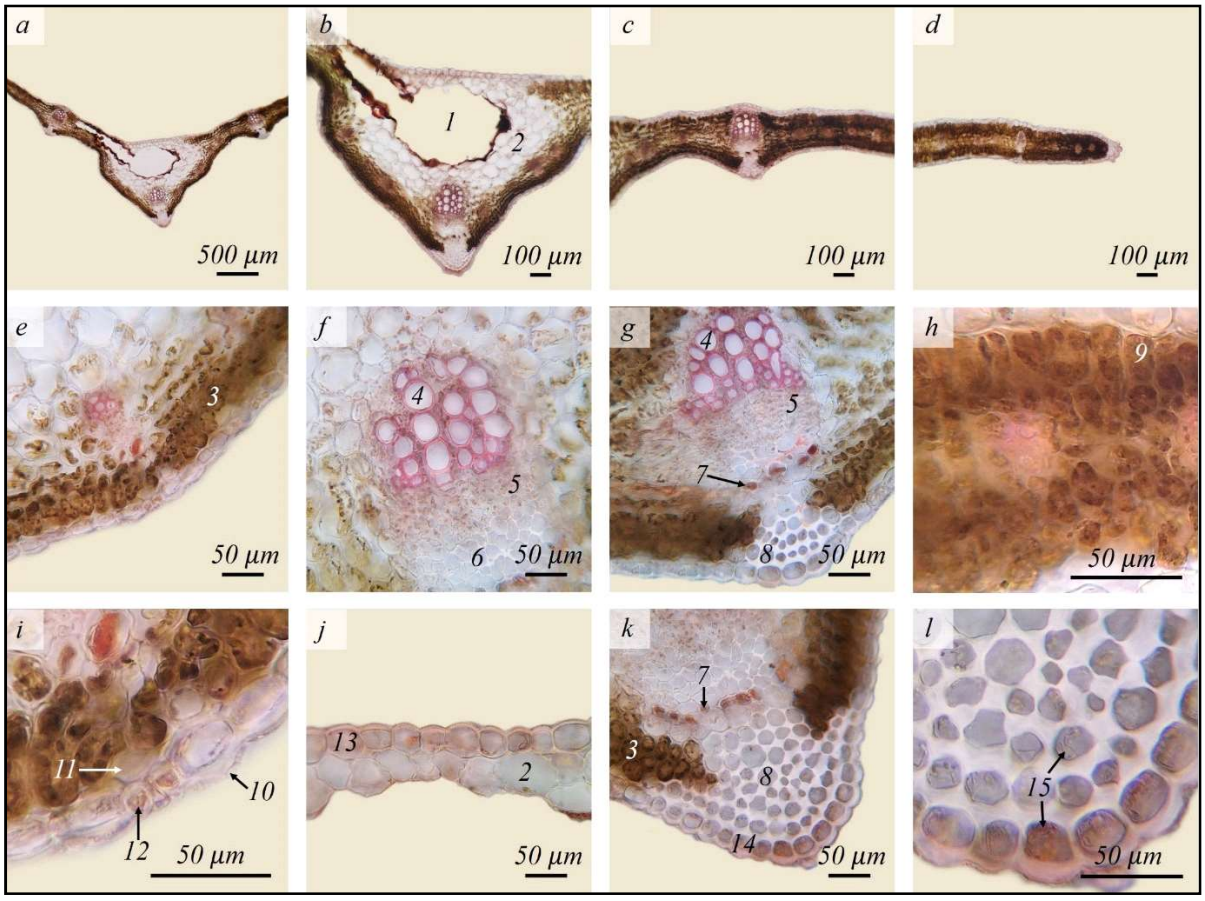

Fig. 6. Transverse section of leaf blade (section thickness: 8 μm): *a* – general view of the leaf blade, *b* – midrib region, *c* – lateral part, *d* – marginal part, *e* – small vascular bundle in the midrib, *f*, *g* – large central and lateral bundles, *h* – pseudoisolateral leaf mesophyll, *i* – epidermal regions containing stoma, *j* – adaxial side of the midrib, *k*, *l* – developed collenchyma tissue on the abaxial side; *1* – air cavity, *2* – parenchyma, *3* – chlorenchyma, *4* – xylem, *5* – phloem, *6* – protosclerenchyma, *7* – laticifers, *8* – collenchyma, *9* – subdifferentiated palisade cells, *10* – cuticle, *11* – sub-stomatal cavity, *12* – guard cells, *13* – adaxial epidermis, *14* – abaxial epidermis, *15* – constitutional substances

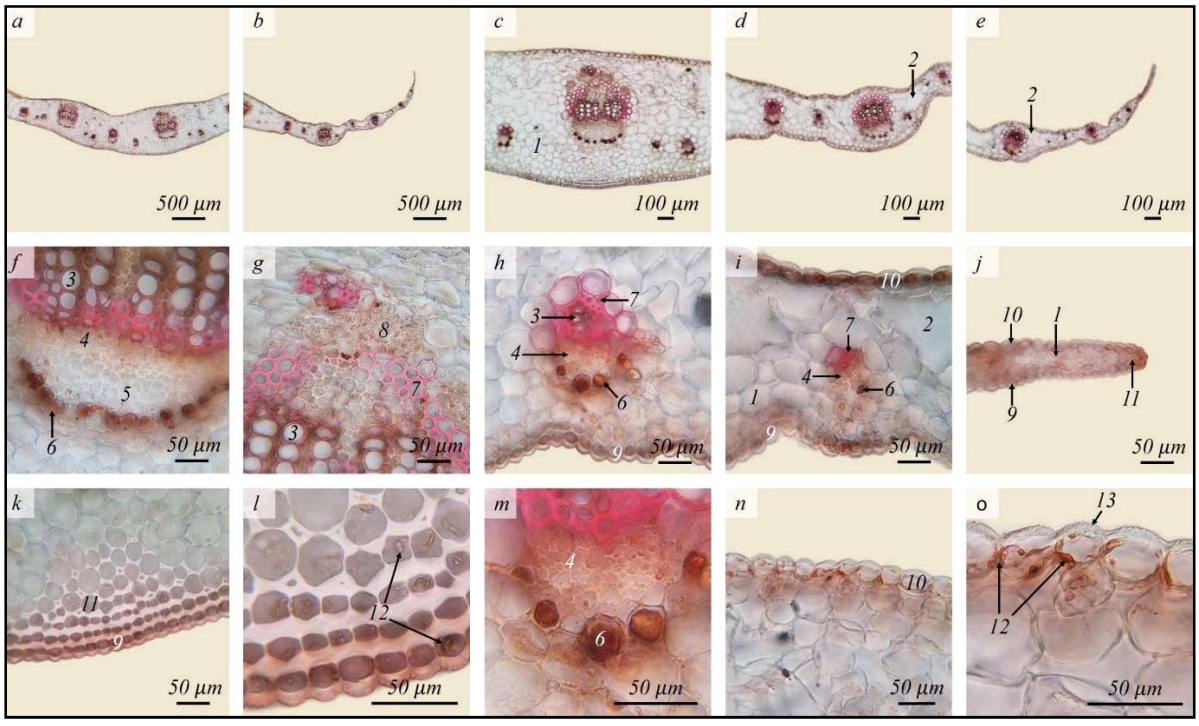

Fig. 7. Transverse section of leaf base (section thickness: 8 μm): *a*, *b* – general view of the leaf base, *c* – central part, *d* – lateral part, *e* – marginal part, *f*, *g* – central vascular bundle and its elements, *h*, *i* – lateral vascular bundles in the parenchyma, *j* – margin of the leaf base, *k*, *l* – collenchyma tissue in the abaxial side, *m* – laticifer cells around the phloema, *n* – adaxial side of the leaf base, *o* – constitutional substances in the epidermis cells; *1* – parenchyma, *2* – aerenchyma, *3* – xylem, *4* – phloem, *5* – protosclerenchyma, *6* – laticifers, *7* – sclerenchyma, *8* – schizogenous secretory canal, *9* – abaxial epidermis, *10* – adaxial epidermis, *11* – collenchyma, *12* – constitutional substances, *13* – cuticle

Table 8
Quantitative characteristic of the stem of *T. pratensis* (n = 15)

Indicators	Mean + SE
Thickness of the cortex	193.73 ± 33.48
Height of epidermal cells	16.58 ± 2.11
Width of epidermal cells	23.05 ± 9.52
Diameter of chlorenchyma cells	21.88 ± 6.86
Diameter of cortex parenchyma cells	30.74 ± 6.58
Height of large vascular bundles	269.81 ± 19.18
Diameter of xylem vessels	26.88 ± 3.18
Diameter of schizogenous secretory canal	82.34 ± 10.02
Diameter of pith parenchyma cells	50.35 ± 14.74

Note: see Table 1.

Rosette. In transverse sections of the rosette, a multi-layered periderm was observed surrounding the cortex. The cortex was relatively thick and exhibited numerous leaf traces extending outward from the central region. Internally, the phloem appeared in radial rows, containing abundant laticifer cells. The phloem was bordered inwardly by a distinct cambial ring, followed by xylem tissue (Fig. 9, Table 9). The xylem vessels were compactly arranged, partially forming rays. Xylem elements also developed within the central pith region of the rosette. Longitudinal sections revealed their lignified walls and distinct perforation plates.

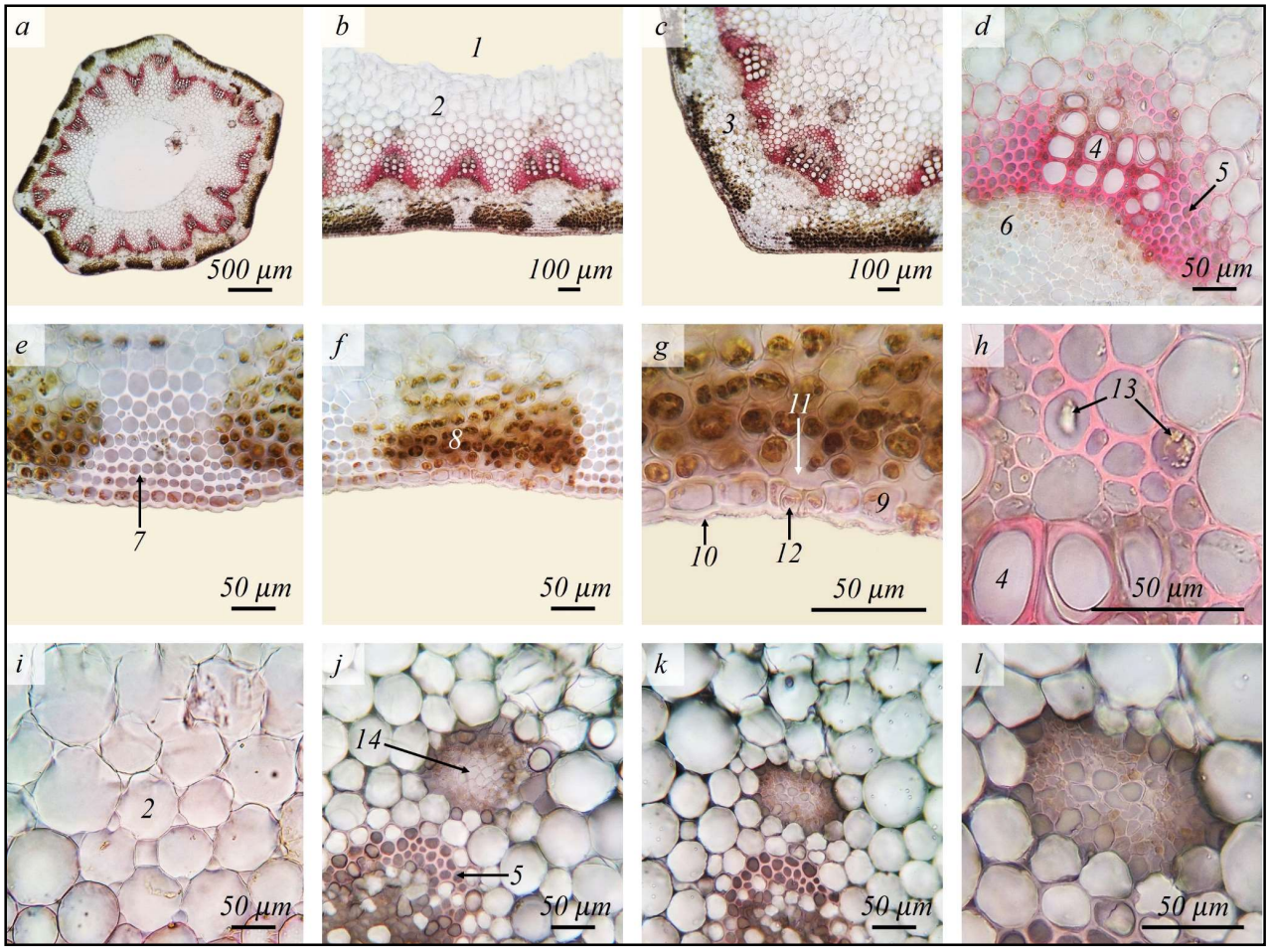

Fig. 8. Transverse section of stem (section thickness: 7 µm): *a* – general view of the stem, *b*, *c* – parts of the stem, *d* – structure of vascular bundle, *e*, *f* – collenchyma and chlorenchyma tissue areas in the peripheral part of the cortex, *g* – stomata on the epidermis, *h* – ergastic substances around the xylem, *i* – pith parenchyma, *j*, *k*, *l* – schizogenous secretory canals in the pith; *1* – pith cavity, *2* – pith, *3* – cortex, *4* – xylem, *5* – sclerenchyma, *6* – phloem, *7* – collenchyma, *8* – chlorenchyma, *9* – epidermis, *10* – cuticle, *11* – sub-stomatal cavity, *12* – guard cell, *13* – ergastic substrances, *14* – schizogenous secretory canal

Table 9
Quantitative characteristic of the rosette of *T. pratensis* (n = 15)

Indicators	Mean + SE
Thickness of the periderm	156.88 ± 12.63
Diameter of cortex parenchyma cells	64.33 ± 11.80
Diameter of xylem vessels	37.26 ± 7.21
Diameter of pith parenchyma cells	46.52 ± 10.02

Note: see Table 1.

Primary Root. The primary root was externally enclosed by a periderm layer. Xylem and phloem tissues were arranged in radial rays. Numerous parenchyma cells were distributed within the cortex, pith, and among the vascular elements (Fig. 10, Table 10). Some parenchyma cells between xylem rays showed evidence of ergastic substance accumulation under microscopic examination. Laticifer cells were located predominantly within the phloem regions.

Table 10
Quantitative characteristic of the primary root of *T. pratensis* (n = 15)

Indicators	Mean + SE
Thickness of the periderm	89.30 ± 9.19
Diameter of parenchyma cells in the phloem region	42.05 ± 14.00
Diameter of parenchyma cells in the xylem region	27.07 ± 7.04
Diameter of xylem vessels	48.93 ± 16.68

Note: see Table 1.

Lateral root. The lateral root retains a primary structure and is surrounded externally by an epiblema, upon which root hairs are distinctly observed. Surrounding the central cylinder, large-sized cells exhibit active development and give rise to a well-defined mesodermal layer. The mesoderm internally abuts the endodermis layer (Fig. 11, Table 11). Microscopic examination revealed brown pigmentation within the joined sheaths of endodermal cells, which may

be associated with the accumulation of biologically active compounds in the medicinally significant species *T. pratensis*. The endodermis encloses a radially organized central cylinder, within which the pericycle is located on the inner side. In the vascular system of the central cylinder, the protoxylem elements are positioned laterally, while metaxylem elements are formed centrally. Phloem tissues were observed grouped around the xylem elements.

Table 11
Quantitative characteristic of the lateral root of *T. pratensis* (n = 15)

Indicators	Mean + SE
Height of epiblema cells	32.02 ± 10.01
Width of epiblema cells	23.90 ± 8.38
Diameter of mesodermal cells	44.24 ± 12.07
Height of endodermis cells	22.06 ± 3.47
Diameter of metaxylem vessels	30.26 ± 8.23

Note: see Table 1.

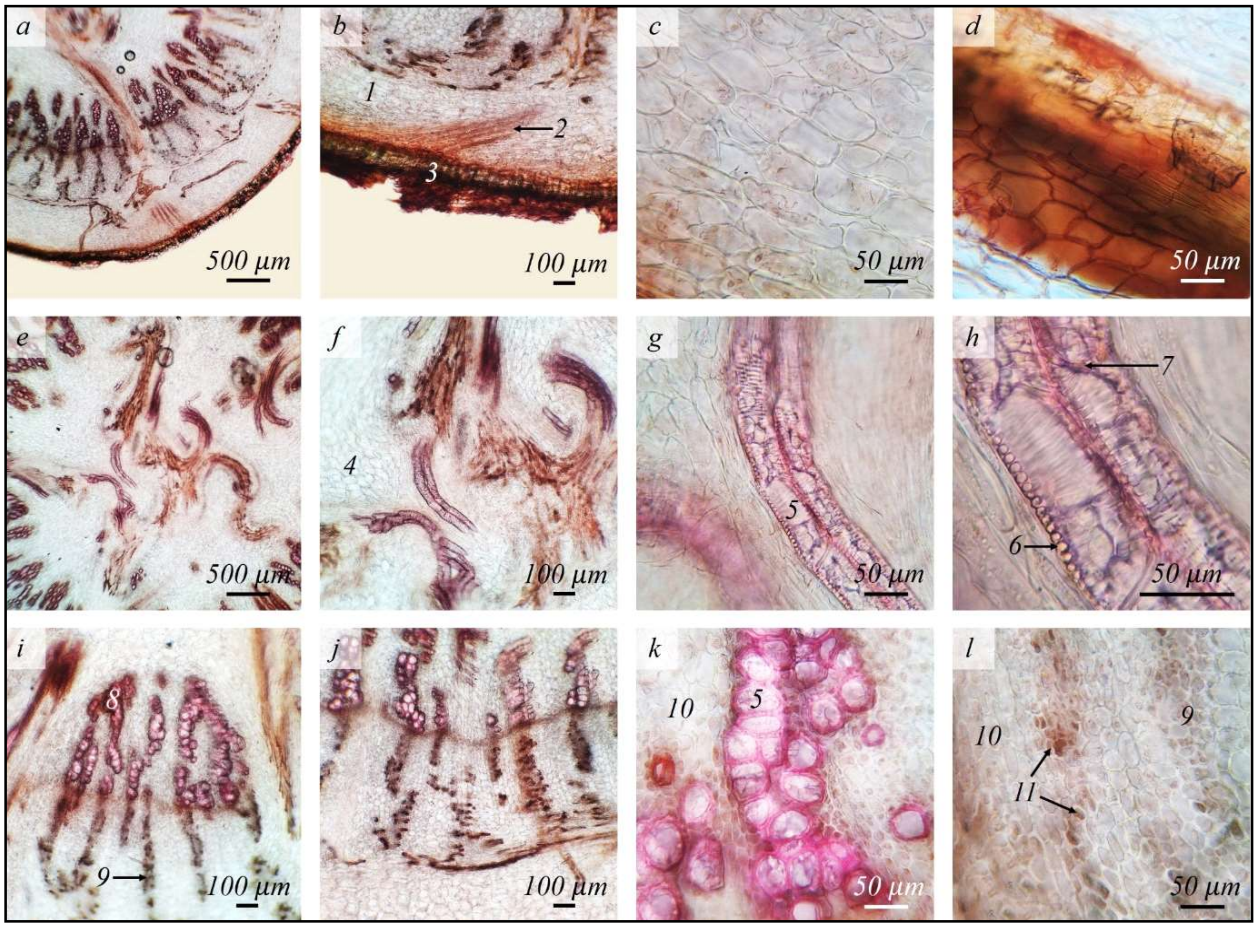

Fig. 9. Transverse section of rosette (section thickness: 8 µm): *a* – part of the rosette, *b* – cortex region, *c* – cortical parenchyma, *d* – periderm, *e*, *f* – pith of the rosette, *g*, *h* – xylem vessels in longitudinal view, *i*, *j* – elements of vascular tissue, *k* – xylem vessels in transverse section, *l* – phloem tissue with laticifers; *1* – cortex, *2* – leaf trace, *3* – periderm, *4* – pith, *5* – xylem vessel, *6* – lignified cell wall, *7* – perforation plate, *8* – xylem, *9* – phloem, *10* – parenchyma, *11* – laticifers

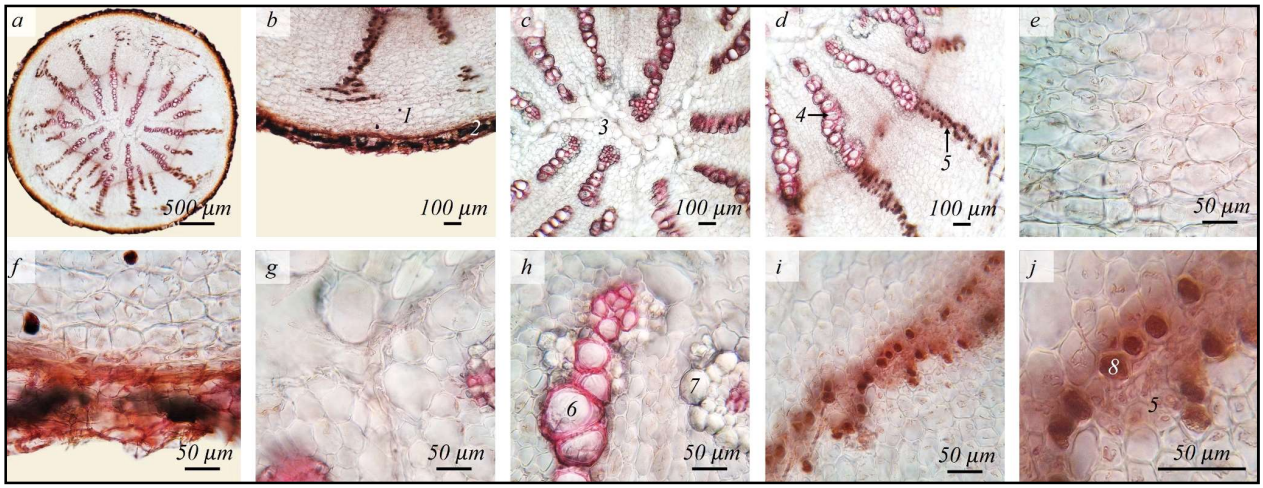

Fig. 10. Transverse section of primary root (section thickness: 7 µm): *a* – general view of root, *b* – cortex, *c* – central region of the root, *d* – vascular tissue, *e* – cortical parenchyma, *f* – periderm, *g* – pith, *h* – ergastic substances in the parenchyma cells surrounding the xylem, *i*, *j* – laticifer cells in the phloem; *1* – cortex, *2* – periderm, *3* – pith, *4* – xylem, *5* – phloem, *6* – xylem vessels, *7* – ergastic substances, *8* – laticifers

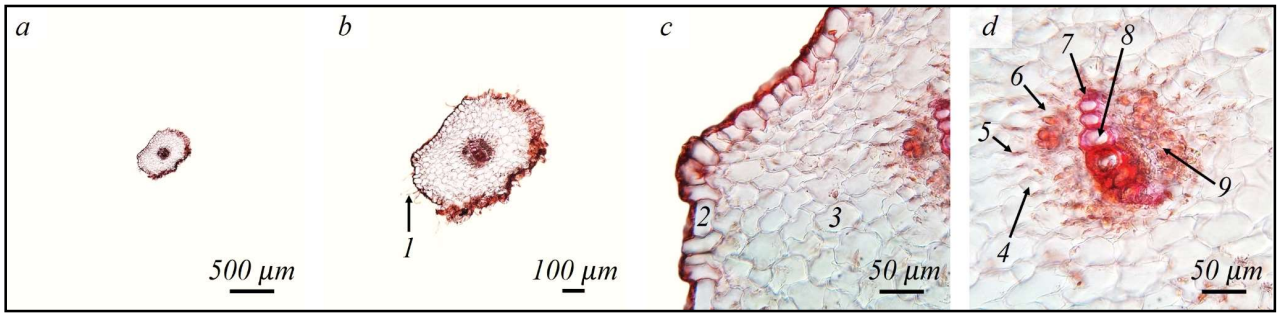

Fig. 11. Transverse section of lateral root (section thickness: 7 μm): *a*, *b* – general view of root, *c* – cortex, *d* – central cylinder of the root; *1* – root hair, *2* – epiblema, *3* – mesodermis, *4* – endodermis, *5* – pigmentation, *6* – pericycle, *7* – protoxylem, *8* – metaxylem, *9* – phloem

Discussion

Anatomical analyses of *Tragopogon pratensis* have revealed a range of stable and diagnostically significant features across its vegetative and generative organs. In the involucral bract, tissues exhibit a compact organization. The pronounced pigmentation of cellular components, along with vacuolization, may reflect intensified metabolic activity. The abundance of laticifer cells adjacent to the vascular bundles and the high accumulation of latex in these regions suggest active secretory function and a defensive role of specialized metabolites. The presence of both glandular and non-glandular trichomes on the abaxial epidermis of the bracts is interpreted as an important adaptive trait involved in transpiration regulation and protective function (Wang et al., 2021).

In the peduncle, a prominent central air canal and chloroplast accumulation in the inter-bundle parenchyma point to a supplementary photosynthetic function and potential hypoxic activity. The large diameter and thick walls of xylem vessels contribute to enhanced hydraulic conductivity and efficient water transport. The richness of parenchymatous cells within the phloem and the accumulation of metabolites further indicate active metabolic exchange in this organ (Elshafie et al., 2023).

The predominance of the pseudoisolateral structure in the leaf mesophyll and the weak development of palisade-type cells are considered important anatomo-functional features that ensure the efficient organization of the photosynthetic parenchyma. The intense intracellular pigmentation and dense chloroplast distribution are linked to high osmotic activity and the accumulation of osmotically active compounds.

In the rosette and root, the presence of large parenchyma cells and a thick periderm layer are stable traits that contribute to mechanical support and protective function. The differentiation and abundance of parenchyma cells in both xylem and phloem, as well as the number and diameter of conducting elements, are primary anatomical features supporting efficient water and nutrient transport in this species. Microscopic investigations confirmed that the localization of laticifers, dimensions of xylem vessels, pseudoisolateral mesophyll structure, and the presence of large air canals are consistent and diagnostically valuable features of *T. pratensis*. These anatomical traits provide a robust basis for species identification and clarification of its systematic position.

The accumulation of pigments in the cell walls of the endodermis in the lateral root, along with the radial organization of the central cylinder, reflects the typical structure of conductive tissue differentiation and is considered an important anatomical criterion ensuring the functional efficiency of water and mineral transport in vegetative organs.

In the generative organs, several significant anatomical markers were identified. The presence of multicellular trichomes and anomocytic stomata in the ligule suggests stable anatomical adaptations contributing to gas exchange and secretion. In the pistil, specific structures of the epidermal cells were observed: oval-shaped protrusions on the style and more pointed projections along the stigma branches suggest mechanical reinforcement and an adaptive role in pollination. The accumulation of drop-like biologically active substances in epidermal cells reflects a high level of secretory activity and secondary metabolite synthesis in the pistil.

In the stamen, the short filament and elongate anther, along with the formation of a specialized apical appendage on the connective tissue, represent reproductive morpho-anatomical features characteristic of the species. Pollen grains display thickened exine forming angular projections with spine-like ornamentation - morphological traits that serve as important diagnostic markers.

Overall, the anatomical traits identified in both generative and vegetative organs of *T. pratensis* characterize the species' unique structural organization and provide a reliable diagnostic basis for its identification and taxonomic positioning.

In a comparative anatomical study of *Tragopogon* species in Turkey, Kaya (2022) analyzed the leaf, stem, and root structures of *T. pratensis* and reported findings that generally correspond with our observations. Similar anatomical characteristics were identified in our investigated specimens, particularly regarding the secretory cells, intervascular sclerenchyma, and latex ducts within the stem. Additionally, Kaya documented the presence of a central cavity in the stem, which was also recorded in our material. However, discrepancies were noted in the structure of the leaf's central vascular bundle. In the micrographs provided by Kaya, the central vein in *T. pratensis* did not exhibit the large aerenchymatous cavity found in our specimens. Interestingly, this structural feature appeared more similar to those observed in *T. pterocarpus* and partially in *T. abbreviatus*, according to Kaya's study. In roots, the periderm layer was reported to be relatively thicker in the Turkish specimens compared to ours, although the overall tissue organization remained consistent.

Futorna et al. (2017), in their anatomical investigation of leaves and stems of three *Tragopogon* species, highlighted the coexistence of xeromorphic and mesomorphic traits. Their study also confirmed the presence of both isolateral and pseudoisolateral mesophyll types. In our research, the presence of a pseudoisolateral mesophyll structure in *T. pratensis* was verified through microscopic analysis, aligning with their observations. Furthermore, Futorna et al. noted the presence of both chloroplast-bearing and non-chlorophyllous parenchyma cells in the stem, which we also identified in our specimens. The authors additionally discussed the localization of schizogenous latex canals within the perimedullary zone or across the entire medullary region of the stem. In our examined specimens of *T. pratensis*, latex canals were situated within the perimedullary zone, consistent with this description, especially considering the formation of a central cavity within the stem.

The study by Azizi et al. (2021) on the pollen morphology of other *Tragopogon* species also supports our palynological findings. In our light microscopy analysis, pollen grains exhibited an oblate-spheroidal shape in equatorial view and a hexagonal outline in polar view – features consistent with the morphological descriptions reported by Azizi et al. (2021).

Conclusion

As a result of the present study, a number of specific anatomical structures with stable and diagnostic significance were identified for the first time in various vegetative and generative organs of *Tragopogon pratensis*. Notable findings include the presence of multicellular

trichomes and anomocytic stomata in the ligules; papillate epidermal cells with distinct projections and accumulation of drop-shaped biologically active compounds in the pistil; a short filament and elongated anther in the stamen, as well as thickened, spiny exine ornamentation forming angular projections on the pollen surface. These characteristics represent structurally and functionally relevant diagnostic features of the species. Microscopic analyses of pollen morphology provide a fundamental reference point for palynomorphological and palynotaxonomic approaches. The pigmentation observed in the cell walls of the endodermis and the radially organized central cylinder in the lateral roots have been characterized for the first time as diagnostic features of the species. Importantly, the pseudoisolateral type of mesophyll in the leaves of *T. pratensis* was recorded for the first time in the flora of Azerbaijan. The current study constitutes the first comprehensive anatomical investigation of *T. pratensis* within the Azerbaijani flora and contributes a critical scientific foundation for clarifying the species' systematic position and expanding the resource of diagnostic features. Thus, this research fills a regional gap in plant anatomical studies and provides baseline reference data for future floristic and pharmacobotanical research. The diagnostic anatomical features identified in *T. pratensis* form a reliable basis for taxonomic categorization, the study of morphological variations, and the development of regional floristic identification keys. Furthermore, the findings hold significance for clarifying phylogenetic relationships and can serve as reference data in comparative anatomo-taxonomic studies. This research is also recommended as a preliminary source for applied investigations in pharmacobotany and ethnobotany, as well as for anatomy-based plant systematics.

This research did not receive any specific grant from funding agencies in the public, commercial, or not-for-profit sectors.

The authors declare that they have no known competing financial interests or personal relationships that could have appeared to influence the work reported in this paper.

References

Abdalla, M. A., & Zidorn, C. (2020). The genus *Tragopogon* (Asteraceae): A review of its traditional uses, phytochemistry, and pharmacological properties. Journal of Ethnopharmacology, 250, 112466.

Aydın, Ö., Coşkuncelebi, K., Gültepe, M., & Güzel, M. E. (2013). A contribution to taxonomy of *Centaurea* including *Psephellus* (Asteraceae) based on anatomical and molecular data. Turkish Journal of Botany, 37, 419–427.

Azizi, H., Sheidai, M., Mozaffarian, V., & Noormohammadi, Z. (2021). Pollen morphology of the genus *Tragopogon* (Asteraceae). Acta Botanica Hungarica, 63(1–2), 31–43.

Belaeva, T. N., & Butenkova, A. N. (2018). Comparative analysis of the leaf anatomy of *Echinacea purpurea* and *E. pallida*. Biosystems Diversity, 26(2), 77–84.

Bell, C. D., Mavrodiev, E. V., Soltis, P. S., Calaminus, A. K., Albach, D. C., Cellinese, N., Garcia-Jacas, N., & Soltis, D. E. (2012). Rapid diversification of *Tragopogon* and ecological associates in Eurasia. Journal of Evolutionary Biology, 25(12), 2470–2480.

Bezerra, L., Callado, C., & Cunha, M. (2020). Does an urban environment affect leaf structure of *Eugenia uniflora* L. (Myrtaceae)? Acta Botanica Brasilica, 34, 266–276.

Bozdağ, B., Kocabaş, O., & Özdemir, C. (2016). A new staining method for hand-cut in plant anatomy studies. Marmara Pharmaceutical Journal, 20(2), 184–190.

da Silva, C. J., de Lima, L. H. F., de Paiva, P. M., Maia, L. M., Rocha, R. E. O., de Souza, P. T. D., & Carvalho, D. A. C. A. (2020). An inexpensive and environmentally friendly staining method for semi-permanent slides from plant material probed using anatomical and computational chemistry analyses. Rodriguésia, 71, e01662018.

Dursun, I., Sağlamtaş, R., Fettahoğlu, K., Zor, M., Sinan, A., Demirci, A., Demir, Y., & Gülçin, İ. (2025). Antioxidant and antimicrobial activities of different extracts of *Tragopogon dubius* and *Tragopogon porrifolium* L. subsp. *longirostris*: Determination of their phytochemical contents by UHPLC-Orbitrap®-HRMS analysis. Food Bioscience, 63, 105604.

Elshafie, H. S., Camele, I., & Mohamed, A. A. (2023). A comprehensive review on the biological, agricultural and pharmaceutical properties of secondary metabolites based – plant origin. International Journal of Molecular Sciences, 24(4), 3266.

Engin, H., Kuzucu, F. C., & Gökbayrak, Z. (2024). Research on the use of different staining techniques in microscopic examination and imaging of wood cuttings. ÇOMÜ Journal of Agricultural Faculty, 12(1), 108–120.

Futorna, O. A., Badanina, V. A., & Zhygalova, S. L. (2017). Ecological-anatomical characteristics of some *Tragopogon* (Asteraceae) species of the flora of Ukraine. Biosystems Diversity, 25(4), 274–281.

Jambor, H., Antonietti, A., Alicea, B., Audisio, T. L., Auer, S., Bhardwaj, V., Burgess, S. J., Ferling, I., Gazda, M. A., Hoeppner, L. H., Ilangovan, V., Lo, H., Olson, M., Mohamed, S. Y., Sarabipour, S., Varma, A., Walavalkar, K., Wissink, E. M., & Weissgerber, T. L. (2021). Creating clear and informative image-based figures for scientific publications. PLOS Biology, 19(3), e3001161.

Kaya, G. (2022). Türkiye'de yayılış gösteren bazı *Tragopogon* L. (Asteraceae) taksonlarının anatomik özellikleri [Anatomical features of some *Tragopogon* L. (Asteraceae) taxa distributed in Türkiye]. Recep Tayyip Erdoğan University (in Turkish).

Kumar, A., Jangid, P. P., Marimuthu, S., Gurav, A. M., Srikanth, N., Mangal, A. K., Venkateshwarlu, B., & Shiddamallayya, N. (2023). Identification and authentication of *Agnimantha* plant species used in Ayurveda on the basis of anatomical and molecular phylogenetic analysis. Plant Science Today, 10(4), 26–38.

Lata, S., Lata, R., Ram, B. R., & Verma, R. S. (2021). Morphological and anatomical adaptations of plants to cope up with environmental stress. Journal of Pharmacognosy and Phytochemistry, 10(6), 142–147.

Liu, W., Zheng, L., & Qi, D. (2020). Variation in leaf traits at different altitudes reflects the adaptive strategy of plants to environmental changes. Ecology and Evolution, 10(15), 8166–8175.

Lv, X., Wang, Y., Wang, X., Zhang, M., Zhang, Y., Zhao, L., & Zhang, X. (2024). Development and anatomy of petals with specialized nectar holder and pollen container in Fumarioideae (Papaveraceae). Planta, 260(1), 21.

Ma, J., Ji, C., Han, M., Zhang, T., Yan, X., Hu, D., Zeng, H., & He, J. (2012). Comparative analyses of leaf anatomy of dicotyledonous species in Tibetan and Inner Mongolian grasslands. Science China. Life Sciences, 55(1), 68–79.

Makruf, M. I., Maryani, & Susandarini, R. (2024). Comparative study of the leaf anatomy of *Dendrobium* species (Orchidaceae) from South Kalimantan, Indonesia and its taxonomic significance. Plant Science Today, 11(2), 742–749.

Poli, L. P., Temponi, L. G., & Coan, A. I. (2017). Floral vasculature and its variation for carpellary supply in *Anthurium* (Araceae, Alismatales). PeerJ, 5, e2929.

Pradhan Mitra, P., & Loqué, D. (2014). Histochemical staining of *Arabidopsis thaliana* secondary cell wall elements. Journal of Visualized Experiments, (87), e51381.

Ramasar, R., Naidoo, Y., Dewir, Y. H., Al-Shahrani, T., & Mendler-Drienyovszki, N. (2025). Seasonal changes in the micromorphology, ultrastructure, and histochemistry of *Carissa macrocarpa* leaves. Notulae Botanicae Horti Agrobotanici Cluj-Napoca, 53(1), 13869.

Rotaru, L. T., Văruț, R. M., Amzoiu, E., Mormoe, M., Nicolaescu, O., Amzoiu, M., & Udrescu, L. (2020). Determination of the antioxidant capacity of *Tragopogon pratensis* species and testing their pancreatic and hepatic regenerative activity. Pharmaceutical Chemistry Journal, 53, 964–970.

Sardarova, A. S. (2024). The anatomical characteristics of the vegetative and generative organs of the medicinal *Silybum marianum* L. spread in the mountainous region of the Lesser Caucasus. Advances in Biology and Earth Sciences, 9(3), 381–388.

Sardarova, A. S. (2025a). Comparative ecological anatomical characteristics of generative and vegetative organs of the medicinally important plant *Fragaria vesca* L. (Rosaceae Juss.) under *in situ* and *ex situ* conditions. Transactions of the Institute of Molecular Biology and Biotechnologies, 9(1), 17–37.

Sardarova, A. S., & Ibadullayeva, S. J. (2025b). Ecological anatomical study of structural-plastic response reactions of the medicinally important species *Laurus nobilis* (Lauraceae) in various ecological conditions. Plant and Fungal Research, 8(1), 23–35.

Sevgi, E., Akkemik, Ü., Yılmaz, H., Sevgi, O., Yılmaz, O., Nomer, N., Baysan, E., & Polat, Z. (2025). Variability in leaf anatomical traits of *Quercus ilex* L. in Eastern Mediterranean and adaptations to the growing environment. Biologia, 80, 1659–1676.

Shahrestani, M. M., Faghir, M. B., & Assadi, M. (2020). Comparative anatomical studies in relation to taxonomy of *Sedum* s.l. (Crassulaceae) in Iran. Turkish Journal of Botany, 44, 281–294.

Simioni, P. F., Emilio, T., Giles, A. L., Freitas, G. V. de, Oliveira, R. S., Setime, L., Vitoria, A. P., Pireda, S., Silva, I. V. da, & Da Cunha, M. (2023). Anatomical traits related to leaf and branch hydraulic functioning on Amazonian savanna plants. AoB Plants, 15(3), plad018.

Soltis, D. E., Mavrodiev, E. V., Brukhin, V., Roalson, E. H., Albach, D. C., Godden, G. T., Alexeev, Y. E., Gitzendanner, M. A., Freeman, C. C., Suárez-Santiago, V. N., & Soltis, P. S. (2023). *Tragopogon pratensis*: Mul-

tiple introductions to North America, circumscription, and the formation of the allotetraploid *T. miscellus*. Taxon, 72(4), 848–861.
Sosnovsky, E., Nachychko, V., Prokopiv, A., & Honcharenko, V. (2021). Leaf anatomical trends in a temperate evergreen dwarf shrub, *Rhododendron myrtifolium* (Ericaceae) along elevational and exposure gradients in the northeastern Carpathian Mountains. Folia Geobotanica, 56, 27–42.
Talebi, S. M., Samiei, M., & Matsyura, A. V. (2025). Morfo-anatomicheskaya mezhvidovaya otsenka razlichnykh populyatsii *Salvia macrosiphon* (Lamiaceae) [Interspecific morpho-anatomical evaluation of diverse populations *Salvia macrosiphon* (Lamiaceae)]. Turczaninowia, 28(2), 181–192 (in Russian).
Uysal, S., Senkardes, I., Mollica, A., Zengin, G., Bulut, G., Dogan, A., Glamočlija, J., Soković, M., Lobine, D., & Mahomoodally, F. M. (2019). Biologically active compounds from two members of the Asteraceae family: *Tragopogon dubius* Scop. and *Tussilago farfara* L. Journal of Biomolecular Structure and Dynamics, 37(12), 3269–3281.
Wang, X., Shen, C., Meng, P., Tan, G., & Lv, L. (2021). Analysis and review of trichomes in plants. BMC Plant Biology, 21(1), 70.